PNAS RESEARCH ARTICLE | NEUROSCIENCE

Neuronal plasticity at puberty in mouse hypothalamic *Kiss1* neurons that control fertility

Yuanxin Zhang[a], Leonie M. Pakulat[a], Szabolcs Takács[b], Lauren Campbell[a], Elisa Galliano[a], Erik Hrabovszky[b], William H. Colledge[a,1], and Susan Jones[a,1]

Edited by Donald Pfaff, Rockefeller University, New York, NY; received May 30, 2025; accepted September 19, 2025

Puberty is a critical transition period to achieve reproductive capacity in all mammalian species. At puberty, hypothalamic *Kiss1* neurons release kisspeptin, stimulating gonadotropin-releasing hormone (GnRH) release and activating the hypothalamic–pituitary–gonadal (HPG) axis. Here, we show that *Kiss1* neurons in the arcuate nucleus of the hypothalamus (*Kiss1*^{ARC}) of female mice undergo profound intrinsic plasticity at puberty. *Kiss1*^{ARC} neurons in brain slices from 3-wk-old mice, when depolarized, typically fire a short high-frequency burst of action potentials before falling silent. This would make them unsuitable for the sustained activity that is required to activate pulsatile GnRH secretion and the HPG axis. At 4 wk of age and after puberty, *Kiss1*^{ARC} neurons can fire a sustained train of action potentials. There is a concomitant hyperpolarization in action potential threshold and postspike minimum voltage and larger medium after-hyperpolarizations (mAHP) and hyperpolarization-induced voltage sags. Transcriptomic profiling showed significant changes in ion channel expression after puberty. Using quantitative PCR, we confirmed changes in genes encoding voltage-gated sodium, calcium, potassium, and cation channels. Blocking hyperpolarization-induced cation channels caused *Kiss1*^{ARC} neurons from postpuberty mice to fire less sustained trains of action potentials. Recordings from *Kiss1*^{ARC} neurons in mice after ovariectomy and 17β-estradiol replacement revealed a critical window of estrogen-dependent plasticity between 3 and 6 wk, which is essential for the maturation of *Kiss1*^{ARC} neurons and the development of their adult electrophysiological activity. This represents an example of sex steroid–dependent plasticity in the mammalian brain at puberty.

kisspeptin | *Kiss1* | arcuate | estrogen | action potential

Significance

Puberty is required for mammals to achieve fertility, which ensures continuation of the species. By the end of puberty, a regular cycle in females allows the periodic release of eggs. This is regulated by hormonal feedback loops between the brain and the gonads. Kisspeptin is a neuropeptide released in the hypothalamus which stimulates puberty and regulates fertility and reproductive capacity in adulthood. Here, we show that during a critical window at the start of puberty, estrogen drives changes in the electrical properties of neurons that release kisspeptin. This makes estrogen essential for the maturation of kisspeptin-releasing neurons at puberty.

Puberty is required for mammals to achieve fertility and reproductive capability to allow continuation of the species. In female mice, the end of puberty is marked by the establishment of a regular estrous cycle which is regulated by hormonal feedback loops within the hypothalamic–pituitary–gonadal (HPG) axis. Pulsatile release of gonadotropin-releasing hormone (GnRH) from the hypothalamus is required for gametogenesis and the production of sex steroid hormones (1). Hypothalamic *Kiss1* neurons release kisspeptins, which are potent stimulators of GnRH secretion after puberty. Mutations in the *Kiss1* receptor *(Kiss1r)* or *Kiss1* genes cause hypogonadotropic hypogonadism in humans (2–5) and in rodent models (3, 6), characterized by reduced gonadotropic hormone concentrations, pubertal failure, and infertility. *Kiss1* neurons in the arcuate nucleus of the hypothalamus (*Kiss1*^{ARC}) project to GnRH neurons from before birth in mice (7) but are generally quiescent until just before puberty. There is currently no mechanistic understanding of how *Kiss1*^{ARC} neurons develop into the generators of GnRH pulsatility at puberty, and in doing so trigger the onset of sexual maturity. This likely represents a critical window of neuronal plasticity in the brain.

The biophysical properties of *Kiss1*^{ARC} neurons in adult mice have been well described using ex vivo brain slices (8–18). Ion channels thought to underlie the electrical properties of adult *Kiss1*^{ARC} neurons include hyperpolarization-activated cyclic nucleotide (HCN) gated channels, voltage-gated Ca^{2+} and K^+ channels, and G protein–coupled inwardly rectifying K^+ channels (15–18). Despite the crucial role of *Kiss1* neurons in puberty, and modest increases in *Kiss1*^{ARC} immunoreactive cells in ewes (19), mice (20), and rats (21), *Kiss1* neuronal plasticity during this critical period of development remains largely unexplored. A strengthening of synaptic contacts between *Kiss1* and GnRH neurons has been reported during puberty in female mice (22), which may reflect an increase in *Kiss1* neuronal activity. Optogenetic stimulation of *Kiss1*^{ARC} neurons in adult mice for at least 2 min at 10 Hz is required to evoke physiological levels of LH release (23). It is not known whether *Kiss1*^{ARC} neurons in prepuberty mice are capable of

Author affiliations: [a]Department of Physiology, Development and Neuroscience, University of Cambridge, Cambridge CB2 3EG, United Kingdom; and [b]Laboratory of Reproductive Neurobiology, Hungarian Research Network, Institute of Experimental Medicine, Budapest 1083, Hungary

Author contributions: Y.Z., L.M.P., E.G., E.H., W.H.C., and S.J. designed research; Y.Z., L.M.P., S.T., E.H., and S.J. performed research; Y.Z., L.M.P., S.T., L.C., E.H., W.H.C., and S.J. analyzed data; and Y.Z., L.M.P., S.T., L.C., E.G., E.H., W.H.C., and S.J. wrote the paper.

The authors declare no competing interest.

This article is a PNAS Direct Submission.

[1]To whom correspondence may be addressed. Email: whc23@cam.ac.uk or sj251@cam.ac.uk.

This article contains supporting information online at https://www.pnas.org/lookup/suppl/doi:10.1073/pnas.2512855122/-/DCSupplemental.

Published October 21, 2025.

sustained neuronal activity. We hypothesized that *Kiss1*^{ARC} neurons would show intrinsic neuronal plasticity (24) across puberty to alter their electrical properties to allow sustained firing after puberty.

Results

Whole-cell patch-clamp recordings were used to compare the action potential (spike) firing properties of *Kiss1*^{ARC} neurons in prepuberty female mice at 3 wk (3 wk) and 4 wk (4 wk) with postpuberty 6 to 9 wk mice (6 to 9 wk; estrus and diestrus). There were no significant differences in *Kiss1*^{ARC} neuron resting membrane potential (RMP), membrane resistance (R_M), or capacitance (C_M) between these age groups (Table 1). Spike firing properties were investigated by injecting incremental current pulses for 500 ms (from a membrane potential of –75 mV, to avoid spontaneous firing). Several parameters of repetitive firing changed around puberty onset (Table 1). The maximum number of spikes significantly increased just prior to puberty, at 4 wk (Fig. 1 *A*–*C*). There was a significant effect of age and current injection on the number of spikes (Fig. 1*B*) with significantly more in *Kiss1*^{ARC} neurons from 4 wk or 6 to 9 wk mice compared with 3 wk mice (Fig. 1*C*). There was a significant effect of age and current injection on the frequency of spike firing (Fig. 1*D*), with firing frequency decreasing significantly by 6 to 9 wk (Fig. 1*E*). The concomitant increase in spike number and decrease in frequency is explained by the increase in the duration of sustained firing after 4 wk (Fig. 1*F*). Firing regularity, measured as the coefficient of variation in the interspike intervals (ISI), was significantly greater in postpuberty mice (Fig. 1*G*). Together, these data suggest that *Kiss1*^{ARC} neurons in 3 wk prepuberty female mice show brief and irregular high-frequency firing, but as they approach puberty their firing patterns stabilize into a lower frequency, regular pattern which they sustain for a longer time.

The current that evoked the maximum number of spikes (Fig. 1*H*) was significantly larger at 4 wk and 6 to 9 wk. Current injections beyond 120 pA led to a progressive decrease in spike number in *Kiss1*^{ARC} neurons of all ages, but this was more pronounced in 3 wk mice, reflected by a smaller current required to reduce the postmaximum spike number by more than 50% compared with 6 to 9 wk (Fig. 1*I*). The ratio of the last to first ISI in the spike train was significantly lower in *Kiss1*^{ARC} neurons from postpuberty mice (Fig. 1*J*), indicating that less spike frequency adaptation (SFA) is occurring. Together, these data suggest that *Kiss1*^{ARC} neurons from 3 wk female mice may be unable to fire sustained trains of action potentials due to depolarization block, SFA, or both, but by 4 wk, this is already changing.

Changes in the firing properties of *Kiss1*^{ARC} neurons at puberty are most likely due to changes in the expression of ion

Table 1. Electrophysiological properties of *Kiss1*^{ARC} neurons (mean ± SE) from pre- and postpuberty female mice

	3 wk	4 wk	6 to 9 wk	*P*-value
Passive properties				
RMP mV	−62.9 ± 1.3	−62.4 ± 1.6	−65.7 ± 1.3	0.22
R_M MOhm	1,118 ± 54	1,020 ± 51.9	1,089 ± 43.4	0.43
C_M pF	35.1 ± 1.3	35.8 ± 1.3	34.5 ± 0.9	0.73
Spike train properties				
Maximum spike number	14 ± 2	22 ± 1.7	24 ± 1.6	**<0.0001**
Maximum frequency Hz	111 ± 6	106 ± 9	75 ± 4	**<0.0001**
Maximum duration ms	354 ± 25	434 ± 12	457 ± 6	**0.0002**
CoV of ISI	0.29 ± 0.04	0.2 ± 0.02	0.18 ± 0.02	**0.049**
Rheobase pA	29 ± 2.5	32 ± 2.4	33 ± 2.4	0.31
SFA %	232 ± 27.1	173 ± 11.4	140 ± 10.3	**0.005**
Maximum current pA	70 ± 5	101 ± 10	125 ± 4	**<0.0001**
mAHP amplitude mV	2 ± 0.2	3.9 ± 0.4	4 ± 0.26	**<0.0001**
OVX + E, Max spike number	13.6 ± 2.9	–	37 ± 3.1	**<0.0001**
OVX + E, Max duration ms	363 ± 40	–	489 ± 1.5	**0.003**
Single spike properties				
Threshold mV	−49 ± 1.2	−53 ± 1.4	−54 ± 0.8	**0.006**
Trough mV	−64 ± 3.5	−84 ± 1.2	−85 ± 1.1	**0.0001**
Peak mV	19 ± 2.5	25 ± 2.7	20 ± 2.1	0.34
Peak to trough time ms	3.1 ± 0.2	2.2 ± 0.1	2.5 ± 0.15	**0.012**
sEPSC properties				
Peak amplitude (pA)	−21.8 ± 2.76	–	−21.9 ± 1.26	0.98
Mean frequency (Hz)	2.34 ± 0.84	–	2.46 ± 0.39	0.56
Rise time (ms)	1.02 ± 0.11	–	1.06 ± 0.07	0.42
Decay tau (ms)	4.07 ± 0.3	–	4.49 ± 0.34	0.38
Voltage sag properties				
Holding potential mV	−75.0 ± 0.78	–	75.6 ± 0.50	0.93
Hyperpolarization, start mV	−103 ± 9.7	–	−107 ± 11.9	0.08
Voltage sag amplitude mV	1.41 ± 0.3	–	6.8 ± 0.4	**0.0001**

For 500 ms data: 3 wk, n = 29 to 39; 4 wk, n = 31 to 32; 6 to 9 wk, n = 34 to 46. For OVX + E at 6 wk, record at 7 wk, n = 10. For OVX at 3 wk, E at 6 wk, record at 7 wk, n = 12. 10 ms data: 3 wk, n = 19; 4 wk, n = 18; 6 to 9 wk, n = 36. For sEPSC properties: 3 wk, n = 15; 6 to 9 wk, n = 20. For voltage sag data: 3 wk, n = 13; 6 to 9 wk, n = 24. *P*-values in bold are significant.

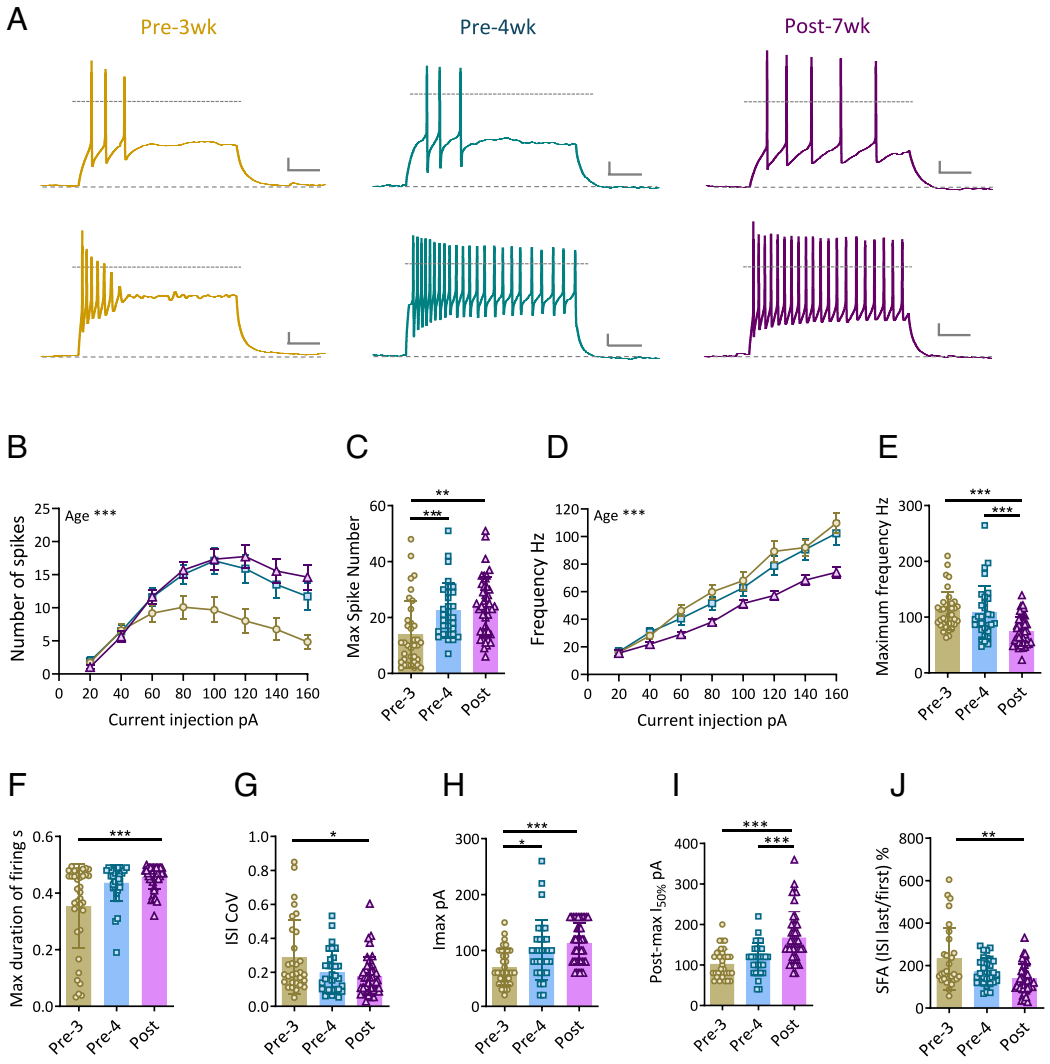

Fig. 1. Repetitive action potential firing properties change in *Kiss1*^{ARC} neurons from female mice at puberty. (*A*) Example traces of repetitive firing during 500 ms current injections in *Kiss1*^{ARC} neurons from a 3-wk-old prepuberty female mouse (*Left*, gold), a 4-wk-old prepuberty female mouse (*Middle*, blue) and a 7-wk-oldpostpuberty female mouse (*Right*, purple: colors apply in all panels). *Top* traces: response to 40 pA injection; *Bottom* traces, response to 100 pA injection. (Scale bar, 10 mV, 100 ms.) (*B*) Number of spikes versus increasing current injection. 3 wk (n = 36, N = 13); 4 wk (n = 31, N = 21); 6 to 9 wk (n = 43, N = 22) in all panels. Mixed model: Current, $P < 0.0001$, F(7,865) = 25; Age, $P < 0.0001$, F(2,850) = 27. Tukey's multiple comparisons show differences between 3 wk and 4 wk ($P < 0.0001$) and 3 wk and 6 to 9 wk ($P < 0.0001$). (*C*) Maximum number of spikes (regardless of current injection). Kruskal–Wallis test, $P < 0.0001$. (*D*) Firing frequency (Hz) versus increasing current injection. Mixed model: Current, $P < 0.0001$, F(7,686) = 73; Age, $P < 0.0001$, F(1.5,524) = 27. Tukey's multiple comparisons show differences between 3 wk and 6 to 9 wk ($P < 0.0001$) and 4 wk and 6 to 9 wk ($P < 0.0001$). (*E*) Maximum spike frequency (regardless of current injection). (*F*) Maximum duration of firing during 500 ms current injection. (*G*) Coefficient of variation in the interspike intervals from the maximum number of spikes. (*H*) Current required to evoke the maximum number of spikes (up to 160 pA). (*I*) Current required to evoke less than half the maximum number of spikes (postmaximum). (*J*) Ratio of the last and first interspike intervals as an indicator of spike frequency adaptation (SFA). All post hoc *P* values: *$P < 0.05$; **$P < 0.01$; ***$P < 0.001$.

channels underlying neuronal excitability, in particular voltage-gated Na^+, K^+, Ca^{2+}, and hyperpolarization-activated nonselective cation channels (Na_V, K_V, Ca_V, and HCN). These changes are reflected in the action potential waveform (25). Incremental current pulses were injected for 10 ms to evoke a single action potential (Fig. 2*A*). The threshold for spike initiation was significantly more hyperpolarized in 6 to 9 wk mice (Fig. 2*B*), but the peak of the spike did not differ (Fig. 2*C*). The minimum voltage after a spike, indicative of a fast afterhyperpolarization (AHP), was significantly more hyperpolarized in *Kiss1*^{ARC} neurons from 4 wk and 6 to 9 wk mice compared with 3 wk mice (Fig. 2*D*), and the time from peak to minimum voltage became significantly faster between 3 to 4 wk (Fig. 2*E*). The voltage response to injections of hyperpolarizing current was unchanging at 3 wk but showed a pronounced voltage sag at 6 to 9 wk (Fig. 2 *F* and *G*). The AHP following a train of spikes, referred to as a medium AHP (mAHP, lasting <300 ms) (26) (Fig. 2*H*) was seen in significantly more postpuberty *Kiss1*^{ARC} neurons (Fig. 2*I*); in neurons with a detectable mAHP, the amplitude was significantly larger in 4 wk and 6 to 9 wk mice (Fig. 2*J*).

To investigate changes in ion channel genes at puberty that could account for the electrophysiological changes, transcriptional profiling was carried out in *Kiss1*^{ARC} neurons from female mice aged either 3 wk or 10 to 12 wk. Out of 196 ion channel transcripts (KEGG BRITE database) expressed in *Kiss1*^{ARC} neurons, 42 changed significantly (*P*.adj ≤ 0.05 by DeSeq2) across puberty (metestrus *vs.* P22, N = 18; proestrus *vs.* P22, N = 41) (Dataset S1). Increases were found in several K_V, Ca_V, and HCN channel subunit genes at both metestrus and proestrus, while decreases were seen in Na_V and other Ca_V and K_V genes (Fig. 3 *A* and *B* and Dataset S1). Transient receptor potential (TRP) cation channels, among which *Trpc5* exhibited the highest expression level (Dataset S1), did not show significant changes. Key changes were

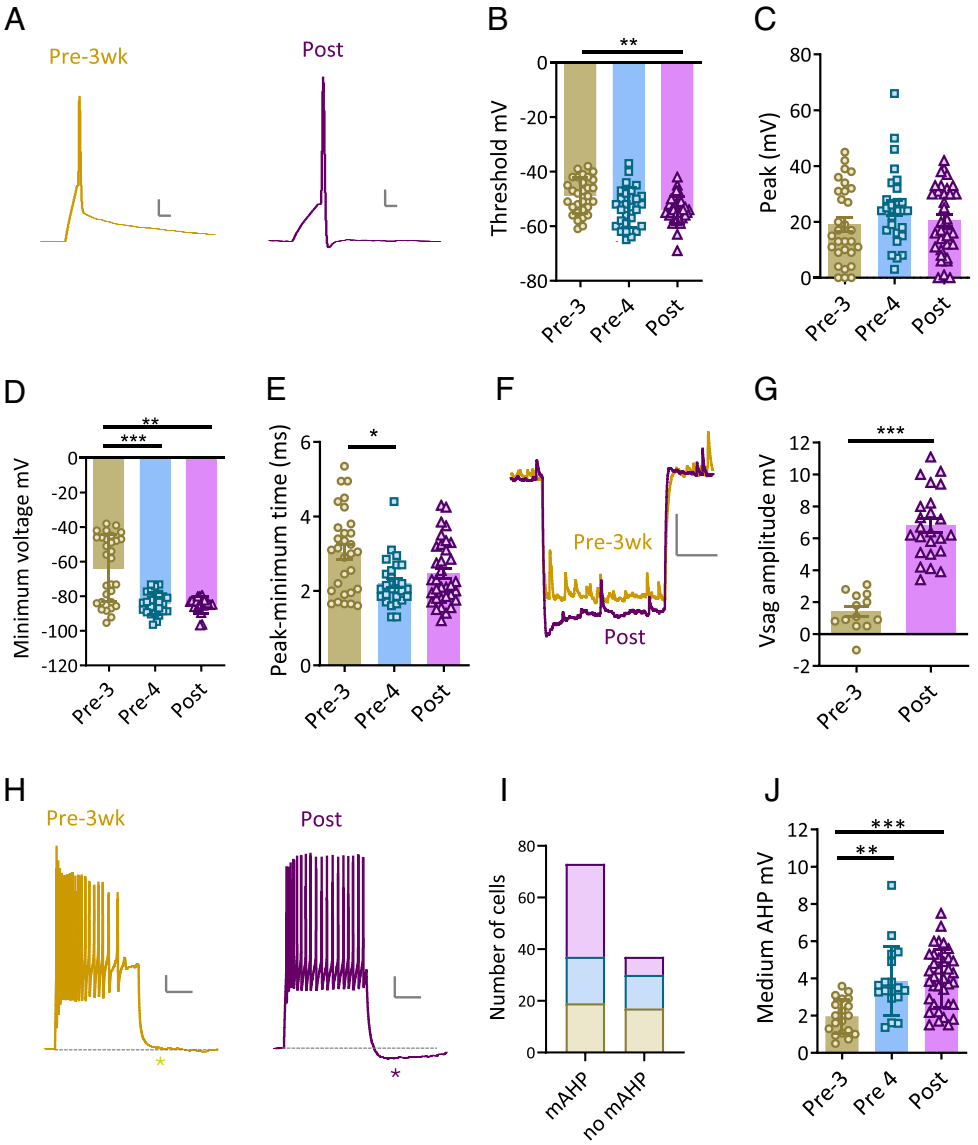

Fig. 2. Action potential waveform, voltage sag, and medium after-hyperpolarization in *Kiss1*^{ARC} neurons change at puberty. (*A*) Example traces of single action potentials during 10 ms current injections in *Kiss1*^{ARC} neurons from a 3 wk prepuberty female mouse *Left*, gold) and a postpuberty female mouse (*Right*, purple); colors apply to all panels. (Scale bar, 10 mV, 10 ms.) (*B*) The threshold for action potential initiation (mV) at 3 wk (n = 30, N = 12), 4 wk (blue, n = 27, N = 18), and 6 to 9 wk (n = 34, N = 18). Kruskal–Wallis test, $P < 0.006$. (*C*) Peak action potential voltage (mV) (n/N as in *B*). (*D*) Minimum voltage following an action potential (n/N as in *B*). Kruskal–Wallis test, $P = 0.0001$. (*E*) Time from the peak of the spike to the minimum voltage (ms) (n/N as in *B*). (*F*) Example traces of the hyperpolarization current-induced slow voltage sag in a postpuberty (purple) but not 3 wk prepuberty (gold) female mouse (scale bars: 10 mV, 1 s). (*G*) Voltage sag amplitude (difference from the start to end of the hyperpolarizing current injection) in 3 wk pre- and postpuberty mice ($P < 0.001$). (*H*) Example traces of the mAHP (*) following a train of action potentials during 500 ms current injections in *Kiss1*^{ARC} neurons from a postpuberty female mouse (*Right*, purple) but not from a 3 wk prepuberty female mouse (*Left*, gold). (Scale bar, 10 mV, 100 ms.) (*I*) The number of *Kiss1*^{ARC} neurons that had a detectable mAHP in 3 wk (gold, n = 19/36), 4 wk (blue, n = 18/31), and 6 to 9 wk (purple, n = 36/43); Chi Squared test, $P = 0.008$. (*J*) Amplitude of the mAHP (Kruskal–Wallis test, $P < 0.0001$). All post hoc *P* values: *$P < 0.05$; **$P < 0.01$; ***$P < 0.001$.

further tested using quantitative PCR (qPCR) in *Kiss1*^{ARC} neurons isolated from female mice aged either 3 wk or 6 to 9 wk (Fig. 3*C* and Table 2). Expression of the *Scn2a* gene, encoding $Na_V1.2$, was significantly lower in postpubertal *Kiss1*^{ARC} neurons, while the genes encoding $Ca_V3.1$ (*Cacna1g*) and HCN1 (*Hcn1*) both increased after puberty. Expression of two K_V genes also changed at puberty, with *Kcnd3* (encoding $K_V4.3$) higher and *Kcnq2* (encoding $K_V7.2$) lower in postpubertal *Kiss1*^{ARC} neurons. Voltage-activated/calcium-regulated large conductance potassium (BK) channels can contribute to fast AHPs; the α subunit gene (*Kcnma1)*, which increased at proestrus in RNA-seq did not show any significant difference in qPCR (Table 2). However, expression of the γ3 subunit gene (*Lrrc55*) was lower in postpubertal *Kiss1*^{ARC} neurons.

Given the robust increase in *Hcn1* (Fig. 3*C* and Dataset S1) and larger voltage sag response (Fig. 2 *F* and *G*) postpuberty, we applied the HCN channel blocker, ZD7288 (ZD), to trains of action potentials in *Kiss1*^{ARC} neurons from postpuberty mice. ZD (50 μM) blocked the voltage sag response (Fig. 3 *D* and *E*), led to a smaller current injection required to evoke the maximum number of spikes (Fig. 3*F*), and reduced the number of spikes as well as the duration of firing compared with the maximum current injection in control (Fig. 3 *G* and *H*). Together, these data suggest that HCN channels in *Kiss1*^{ARC} neurons of postpuberty mice contribute to their ability to fire sustained trains of action potentials, most likely together with other ion channels.

A change in excitatory synaptic drive to *Kiss1*^{ARC} neurons at puberty could lead to changes in action potential firing and

potentially drive the reactivation of the HPG axis at puberty. To investigate this, spontaneous excitatory postsynaptic currents (sEPSCs) were recorded in *Kiss1*^{ARC} neurons from mice aged 3 wk and 6 to 9 wk (estrus and diestrus combined). There was no significant difference in the amplitude, frequency, or kinetics of sEPSCs (Table 1) and no change in the expression of *Gria2* (Table 2), which encodes the GLUA2 AMPA receptor subunit, providing no evidence for a change in excitatory drive to *Kiss1*^{ARC} neurons at puberty.

Estrogen levels begin to rise prior to puberty and fluctuate during the estrous cycle after puberty (27, 28). If estrogen is required for the mature firing properties of *Kiss1*^{ARC} neurons after puberty, then differences might be expected at different stages of the estrous cycle when circulating estrogen levels differ. There was no significant difference between estrus and diestrus in maximum spike number or frequency of firing in response to 500 ms current injections (Fig. 4 *A* and *B*). To determine whether estrogen is necessary to maintain postpuberty firing properties, the ovaries were removed at the end of puberty (6 wk OVX) and recordings were carried out at 7 to 8 wk. Implants of 17β-estradiol (+E) that should provide a constant diestrus level of hormone (29) were given at 6 wk, to mitigate the hyperexcitability of *Kiss1*^{ARC} neurons caused by removing estrogen-mediated negative feedback. In mice having OVX + E at 6 wk, the maximum number of spikes was significantly larger than both 3 wk and 6 wk intact mice; this likely reflects residual hyperexcitability caused by OVX, even with the 17β-estradiol implant (Fig. 4*C*). Note that OVX + E at 6 wk mice do not resemble 3 wk intact mice, indicating that OVX + E at 6 wk does not prevent intrinsic plasticity occurring in *Kiss1*^{ARC} neurons. The duration of firing was significantly different in OVX + E at 6 wk mice compared with intact 3 wk and 6 to 9 wk mice (Fig. 4*D*) but had a similar mean value to intact 6 to 9 wk mice.

To determine whether the rise in estrogen at puberty is necessary for the maturation of *Kiss1*^{ARC} neurons, ovaries were removed before puberty onset (3 wk OVX) and recordings were carried out at 7 to 8 wk. 17β-estradiol implants were given at 6 wk; thus, mice undergoing OVX at 3 wk had no circulating estrogen between 3 to 6 wk. In these mice, the maximum number of spikes recorded at 7 to 8 wk in *Kiss1*^{ARC} neurons was the same as in 3 wk intact mice, but significantly lower than the maximum number of spikes in 6 to 9 wk intact mice (Fig. 4*E*), while the duration of firing was intermediate between 3 wk and 6 to 9 wk intact mice (Fig. 4*F*). The number of spikes per current injection in *Kiss1*^{ARC} neurons from 7 to 8 wk mice that had OVX at 3 wk compared with OVX at 6 wk is shown in Fig. 4*G*; there was a significant effect of both age and current injection, with profoundly lower numbers of spikes in mice having OVX at 3 wk. This suggests that OVX at 3 wk, with the resulting absence of estrogen between 3 to 6 wk, prevents the intrinsic plasticity occurring in *Kiss1*^{ARC} neurons at puberty, such that *Kiss1*^{ARC} neurons fail to achieve their mature physiological phenotype.

Table 2. Ion channel gene expression determined using qPCR analysis of isolated *Kiss1*^{ARC} neurons from 3w or 6 to 9w female mice (mean ± SE)

Gene	Encodes	3 wk	6 to 9 wk	*P*-values
Scn2a (N = 4,6)	$Na_V1.2$	1.02 ± 0.1	0.62 ± 0.06	**0.019**
Cacna1g (N = 5,5)	$Ca_V3.1$	1.25 ± 0.48	3.18 ± 0.61	***0.055***
Cacna1i (N = 2,4)	$Ca_V3.3$	1.02 ± 0.20	0.50 ± 0.14	*0.133*
Kcnc1 (N = 5,5)	$K_V3.1$	1.11 ± 0.27	0.82 ± 0.20	0.42
Kcnd3 (N = 5,5)	$K_V4.3$	1.07 ± 0.2	3.38 ± 0.51	**0.008**
Kcnq2 (N = 5,5)	$K_V7.2$	1.01 ± 0.08	0.64 ± 0.06	**0.016**
Kcnq5 (N = 4,5)	$K_V7.5$	1.14 ± 0.35	1.05 ± 0.21	>0.99
Kcnma1 (N = 4,4)	BKα	1.07 ± 0.21	1.24 ± 0.17	0.69
Lrrc55 (N = 5,5)	BKγ3	0.90 ± 0.16	0.27 V 0.08	**0.016**
Kcnn2 (N = 4,4)	SK2	1.03 ± 0.13	0.72 ± 0.26	0.48
Kcnn3 (N = 4,4)	SK3	1.25 ± 0.53	1.67 ± 0.99	>0.99
Hcn1 (N = 5,5)	HCN1	1.38 ± 0.49	4.83 ± 0.91	**0.016**
Hcn2 (N = 5,5)	HCN2	1.38 ± 0.44	1.71 ± 0.45	0.69
Hcn3 (N = 5,5)	HCN3	1.33 ± 0.6	0.83 ± 0.12	>0.99
Hcn4 (N = 4,5)	HCN4	1.09 ± 0.25	1.2 ± 0.26	0.90
Gria2 (N = 5,4)	GLUA2	1.08 ± 0.19	1.14 ± 0.06	0.9

N refers to the number of mice (3 wk, 6 to 9 wk). All tests of 3 wk versus 6 to 9 wk: Mann–Whitney. *P*-values in bold are significant.

Discussion

Neuronal plasticity is associated with critical periods of brain development, and an important developmental period for the survival of the species is puberty, when individuals achieve fertility and reproductive capacity. We report evidence that hypothalamic *Kiss1*^{ARC} neurons, that control puberty and fertility, undergo intrinsic neuronal plasticity at puberty in female mice, including changes in action potential firing properties and changes in Na_V, Ca_V, K_V, and HCN ion channel genes. Prior to puberty, in 3-wk-old mice, *Kiss1*^{ARC} neurons have firing properties that would make them unsuitable for the sustained activity shown to be required for pulsatile LH secretion (23). Consistent with this, very few LH pulses are detected at weaning (3 wk) in mice, but this increases during the juvenile period (3 to 4 wk) (30). The changes we have identified could endow postpuberty *Kiss1*^{ARC} neurons with a mature physiological phenotype that allows them to perform their role as activators of the HPG axis (31) by firing in a sustained manner. Furthermore, optogenetic stimulation of GnRH neurons for 2 min at 10 Hz also elicits LH pulses resembling physiological activity (32); thus sustained activity of both *Kiss1* and GnRH neurons is associated with pulsatile hormone release in the HPG axis. Interestingly, the change in firing is already apparent by 4 wk. Thus, intrinsic plasticity of action potential firing in *Kiss1*^{ARC} neurons between 3 to 4 wk, just prior to puberty onset and requiring ovarian estrogen, could be the trigger for the essential sustained activity in both *Kiss1*^{ARC} and GnRH neurons.

The passive and active membrane properties of *Kiss1*^{ARC} neurons are well characterized in adult female mice (18). They are small neurons with high input resistance and a resting membrane potential of −50 to −75 mV (8–12, 15, 33); reviewed by (9, 14, 18). Most of our recordings were carried out in neurons from gonadally intact pre- and postpuberty female mice; no differences in capacitance, input resistance, or resting membrane potential were

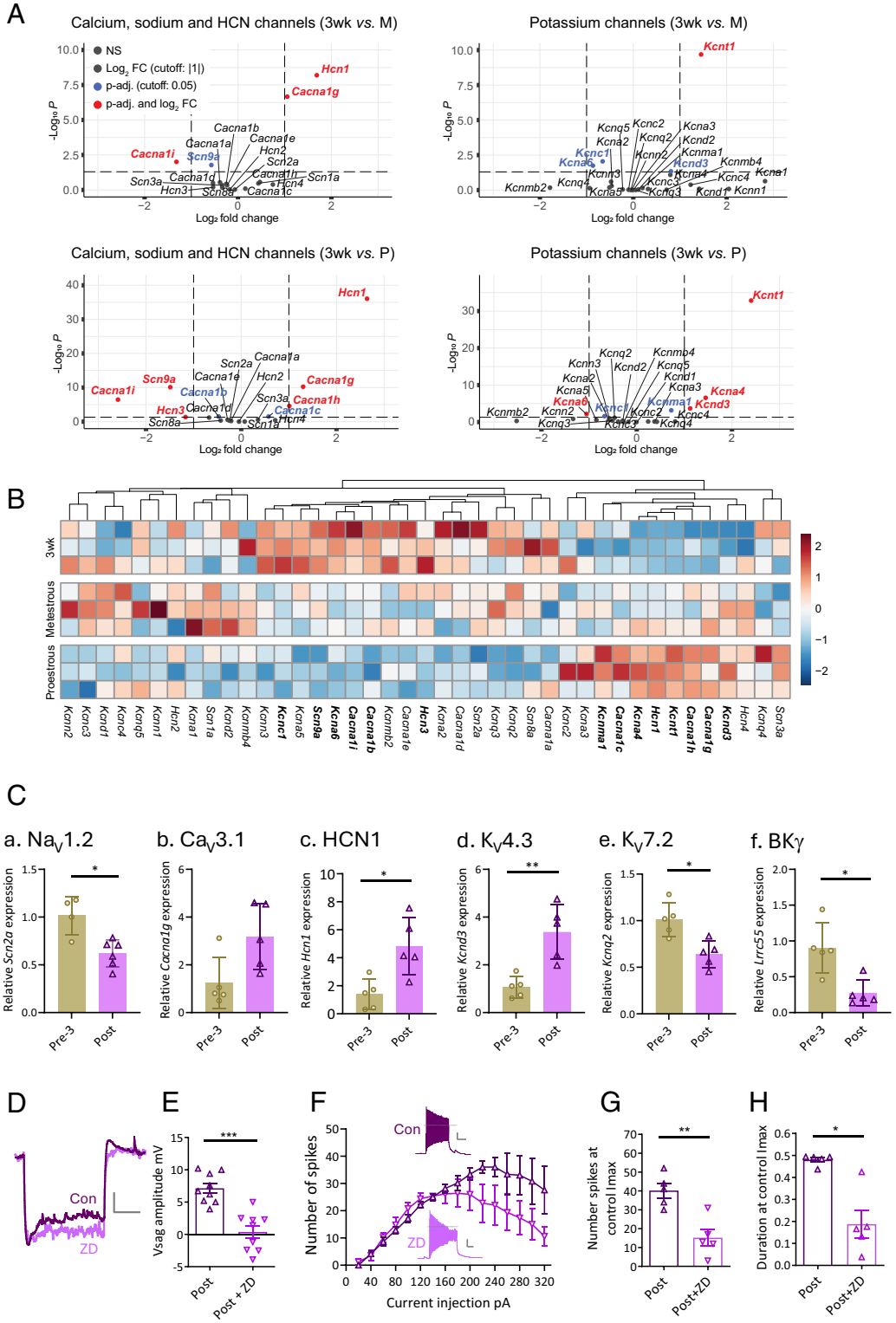

Fig. 3. Changes in ion channel gene expression in *Kiss1*^{ARC} neurons of female mice at puberty. (*A*) Volcano plots showing expression differences in genes encoding calcium, sodium, and HCN channel subunits (*Left* panels) and potassium channel subunits (*Right* panels) in *Kiss1*^{ARC} neurons between prepuberty (3 wk) and postpuberty (10 to 12 wk) mice in either metestrus (M, *Top* panels) or proestrus (P, *Bottom* panels). (*B*) Heat map illustrating relative expression levels of the ion channel transcripts from *A*. Symbols in bold indicate statistically different changes (*P*.adj < 0.05 by DESeq2 analysis). (*C*) Relative expression (compared to housekeeping gene, TATA box binding protein gene *Tbp;* no significant change at puberty, *P* = 0.85) of genes encoding $Na_V1.2$ (*Scn2a*), $K_V4.3$ (*Kcnd3*), $K_V7.2$ (*Kcnq2*), HCN1 (*Hcn1*), and the γ3 subunit of the BK channel (*Lrrc55*) were significantly different while $Ca_V3.1$ (*Cacna1g*) was not quite significant (*P* = 0.056) in qPCR analysis of isolated *Kiss1*^{ARC} neurons from 3 wk prepuberty (gold, n = 5 mice) and 6 to 9 wk postpuberty (purple, n = 5 mice) females (Mann–Whitney *U* test in all cases). All post hoc *P* values: **P* < 0.05; ***P* < 0.01; ****P* < 0.001. (*D*) Example traces showing the voltage sag responses to hyperpolarizing current injections in postpuberty mice in control and in the presence of the HCN channel blocker, ZD7288 (50 μM). (Scale bar, 10 mV, 1 s.) (*E*) Voltage sag amplitude in control and then in ZD7288 (n = 9, N = 5; *P* < 0.001). (*F*) Number of spikes versus increasing current injection in control and ZD7288 from postpuberty mice (n = 5, N = 5). Imax in control: 264 ± 16 pA; Imax in ZD: 192 ± 24 pA, *P* = 0.02, paired *t* test. The inset shows spike trains in response to a maximum current injection (con) and the response to the same current injection in ZD; (Scale bar, 10 mV, 200 ms.) (*G*) Number of spikes in response to the current injection evoking the maximum number of spikes in control (40 ± 3.8) and then following ZD7288 application (15 ± 4.6; *P* < 0.01, paired *t* test). (*H*) Duration of firing in response to the current injection evoking the maximum number of spikes in control (480 ± 10 ms) and then following ZD7288 application (187 ± 64 ms; *P* < 0.05, paired *t* test).

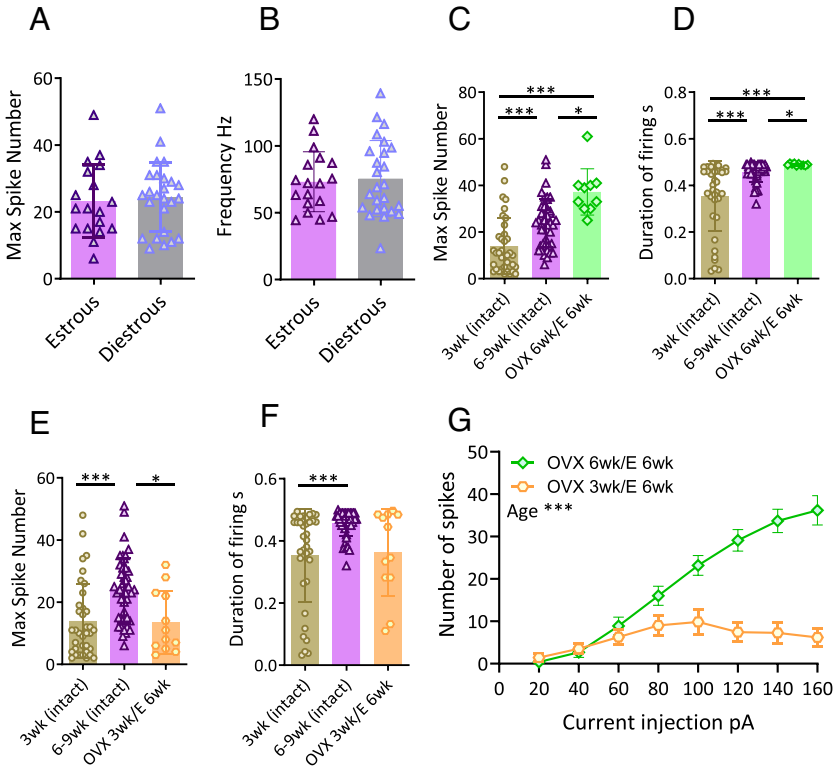

Fig. 4. Intrinsic plasticity in *Kiss1*^{ARC} neurons is prevented by OVX at 3 wk. (*A* and *B*) Maximum number of spikes ($P = 0.7$) and maximum firing frequency (Hz; $P = 0.86$) in *Kiss1*^{ARC} neurons from 6 to 9 wk postpuberty female mice in the estrous phase (lilac bars) or diestrous phase (gray bars) of the estrous cycle). (*C* and *D*) Maximum spike number and maximum duration of firing in mice that had OVX at 6 wk, compared with 3 wk intact and 6 to 9 wk intact mice (*C* and *D*, Kruskal–Wallis, $P < 0.0001$). (*E* and *F*) Maximum spike number and Maximum duration of firing in mice that had OVX at 3 wk compared with intact 3 wk and 6 to 9 wk mice (*E*, Kruskal–Wallis, $P < 0.0001$; *F*, Kruskal–Wallis, $P = 0.0004$). (*G*) The number of spikes versus current injection in *Kiss1*^{ARC} neurons from mice that had OVX at 3 wk (orange hexagons, n = 12) or at 6 wk (green diamonds, n = 10). In both OVX groups, 17β estradiol implants were given at 6 wk. Mixed model: Current, $P < 0.0001$, F(7,167) = 14; Age, $P < 0.0001$, F(1,167) = 77. All post hoc *P* values: *$P < 0.05$; **$P < 0.01$; ***$P < 0.001$.

observed. *Kiss1*^{ARC} neurons show either no spontaneous action potential firing or irregular firing with highly variable frequency (0.5 to 5 Hz) (8–10, 15, 34). To our knowledge, only one study describes spontaneous action potential firing of prepubertal *Kiss1*^{ARC} neurons, showing that 70% are silent while 30% fire irregularly at ~2.5 Hz (10). Many electrophysiological studies of *Kiss1*^{ARC} neurons have been done in adult OVX or OVX + E female mice to capture their phenotype when there is no cycling of sex hormones. In *Kiss1*^{ARC} neurons from OVX mice, action potential threshold (9, 33), duration of firing (33), firing frequency (12), and spontaneous action potential firing (34) are all significantly higher compared to OVX + E or intact mice. To standardize measurements of firing between pre- and postpuberty mice, we held the membrane potential at −75 mV and delivered depolarizing current injections for 500 ms. In these recordings, *Kiss1*^{ARC} neurons showed a dramatic change in firing properties, from high-frequency short duration and irregular firing in mice aged 3 wk to sustained firing at lower frequency with greater regularity by 6 to 9 wk, with an increase in the maximum number of spikes already apparent by 4 wk, suggesting that the process of maturation begins between 3 to 4 wk.

The short duration of firing at 3 wk could be explained by depolarization block: a period of silence in the depolarized neuron due to inactivation of Na_V channels (35). Consistent with this, spike number decreased with increasing depolarization. There might also be SFA: initially high-frequency firing slowing down during a train of spikes, sometimes stopping altogether (36). The ratio of the last/first interspike intervals was greater in 3 wk mice compared with 6 to 9 wk. In general, there was more variability in all parameters measured in *Kiss1*^{ARC} neurons from 3 wk mice, suggesting that individual neurons are developing at different rates with some achieving a mature phenotype earlier than others. Nevertheless, the overall population was significantly different than in 6–9 wk mice. The changes in firing properties could allow postpuberty *Kiss1*^{ARC} neurons to fire sustained trains of action potentials which would be amenable for neuropeptide modulation by NKB and dynorphin, generating burst firing that results in pulsatile release of kisspeptin and thus GnRH and LH (37).

The expression of several genes encoding ion channels also changed at puberty. The decrease in *Scn2a* (encodes $Na_V1.2$) might seem paradoxical alongside an increase in spike number at puberty, but $Na_V1.2$ channels have been shown to cause neurons to fire fewer spikes (38). Genes encoding two "low voltage activated" (LVA) ion channels increased at puberty: *Cacna1g* (encodes a transient, inactivating "T-type" Ca_V channel, $Ca_V3.1$) and *Kcnd3* (encodes a rapidly activating and inactivating K_V channel, $K_V4.3$) (39, 40). T-type Ca_V channels can couple to calcium-activated potassium channels to generate stable, pacemaker firing in other brain neurons (41). Hyperpolarized spike thresholds (for LVA channels), larger AHPs (for removal of channel inactivation), and larger voltage sags (to depolarize from the AHP) in postpuberty *Kiss1* neurons could facilitate the activation of $Ca_V3.1$ and $K_V4.3$ channels.

These changes in gene expression might underlie the hyperpolarized spike threshold and minimum postspike voltage in postpuberty mice. Ion channels that contribute to fast AHPs include K_V3 and BK channels. A decrease in *Kcnc1* (encoding $K_V3.1$) was detected with RNA-seq but not qPCR. An increase in *Kcnma* (encoding BKα) was seen at proestrus in RNA-seq but not in qPCR, while the *Lrrc55* gene (encoding γ3) was decreased. BKγ

subunits facilitate BK channel activation at resting voltage and calcium levels (42); this might be important at 3 wk, when *Cacna1g* expression is lower. Increased *Cacna1g* after puberty could provide LVA calcium influx to facilitate BK channel activation, possibly making γ3 redundant. BK channels can have both excitatory and inhibitory effects on spike firing and maintain the required level of firing (43); possibly they are less effective at this in prepuberty neurons. Interestingly, RNA-seq detected a strong increase in *Kcnt1* (encoding a sodium-activated potassium channel); this could also contribute to steadier spike firing.

Ion channels contributing to the mAHP include small conductance calcium-activated K^+ channels and K_V7 channels (26); their genes did not change in RNA-seq, although *Kcnq2* decreased in qPCR. Either these channels do not contribute to the increased mAHP postpuberty, or their expression is below our level of detection. HCN channels can contribute to the depolarization following a mAHP; *Hcn1* gene expression increased at puberty and hyperpolarization-induced voltage sag responses were larger postpuberty. Functional HCN channels have been demonstrated in adult mouse (44) and guinea pig (45) *Kiss1*^{ARC} neurons; here, we show they are negligible at 3 wk. Combined with the increases in *Cacna1g* and *Kcnd3*, HCN channels might play a critical role in mature *Kiss1* neurons in coupling the rebound from hyperpolarization to activation of LVA channels. Supporting this idea, blocking HCN channels that underlie the voltage sag led to a reduction in sustained firing in postpuberty *Kiss1*^{ARC} neurons, but did not replicate the 3 wk spike train phenotype; this likely requires removal of several ion channels. Future work could explore this using pharmacology and/ or genetic deletion.

The changes seen at puberty could be explained by the rise in estrogen levels after puberty onset. No differences in repetitive firing properties were seen between estrus and diestrus mice, and *Kiss1*^{ARC} neurons from mice that were OVX + E at 6 wk more closely resembled intact 6 to 9 wk mice, indicating that the maturation of firing properties was not prevented by OVX + E at 6 wk. In contrast, in mice that were OVX at 3 wk and given 17β-estradiol at 6 wk, *Kiss1*^{ARC} neurons showed firing properties similar to gonadally intact 3 wk mice, suggesting that the development of intrinsic plasticity was prevented by OVX at 3 wk and this could not be restored by estrogen replacement at 6 wk. Thus, estrogen at the start of puberty opens a window of plasticity in *Kiss1*^{ARC} neurons. LH levels were not measured in either intact or OVX + E mice, so we cannot relate the changes in *Kiss1*^{ARC} neuron firing at puberty to the release of GnRH and LH; however, the requirement for sustained *Kiss1*^{ARC} neuron activity to evoke physiological levels of LH release (23) suggests that estrogen-dependent neuronal plasticity at puberty could be important for pulsatile hormone release. Future work should investigate this.

In conclusion, we have demonstrated a sex-steroid–dependent critical window for neuronal plasticity of spike firing and ion channel gene expression in hypothalamic *Kiss1* neurons that control fertility. This is consistent with the broader evidence for sex steroid–dependent structural and functional plasticity in the brains of both animals and humans at puberty (46).

Materials and Methods

Animals and Brain Slice Preparation. Experiments were carried out under the UK Home Office Animals (Scientific Procedures) Act 1986, following ethical review by the University of Cambridge. Female mice used in this study were bred from heterozygous *Kiss1-Cre* (47) and homozygous tdTomato mice [*Gt(ROSA)26Sor*$^{tm9(CAG\text{-}tdTomato)Hze}$/J; stock #007909; The Jackson Laboratory] to visualize *Kiss1* neurons. It has previously been shown that 90% of tdTomato neurons express kisspeptin in these mice (47). Mice were group-housed by sex in open-top cages (12:12 h dark/light) with free access to food and water. Puberty was defined as the initial opening of the vaginal canal (VO), and prepuberty mice were either 3 wk (3 wk: P22-P26) or 4 wk (4 wk: P28-P34) of age, while postpuberty mice were 6 to 9 wk old (6 to 9 wk: P43 to P62) with a regular estrous cycle, determined by cytological examination of vaginal lavages (48). Mice were killed by cervical dislocation and brains removed and submerged in ice-cold solution containing (mM): 206 sucrose, 2.5 KCl, 1.25 NaH_2PO_4, 26 $NaHCO_3$, 20 glucose, 5 $MgCl_2$, and 1 $CaCl_2$, pH 7.4 with 95% O_2/5% CO_2. Coronal brain slices (250 μm) through the ARC were prepared using a Campden 7000smz Vibrating Microtome (Campden Instruments, UK) then transferred to an incubation chamber containing (mM): 119 NaCl, 2.5 KCl, 1.25 NaH_2PO_4, 26 $NaHCO_3$, 20 glucose, 5 $MgCl_2$, 2 $CaCl_2$ at 30 °C, saturated with 95% O_2 and 5% CO_2, and left undisturbed for at least 60 min.

Electrophysiology. Brain slices containing *Kiss1*^{ARC} neurons expressing tdTomato were perfused with oxygenated solution (as above but with 1 $MgCl_2$ and 20 glucose) at 30 ± 2 °C. The intracellular pipette solution contained (mM): 120 K^+-Gluconate, 9 KCl, 3.5 $MgCl_2$, 4 NaCl, 10 HEPES [4-(2-hydroxyethyl)-1-piperazineethanesulfonic acid], 4 Na_2ATP, 0.4 Na_3GTP, 0.5 $CaCl_2$, 0.3 EGTA [Ethylene glycol-bis(2-aminoethylether)-*N,N,N′,N′*-tetra-acetic acid], pH 7.2 to 7.3, 270 to 285 mOsm. Resting membrane potential (RMP) was determined at the start of each experiment, and series resistance (R_S), membrane resistance (R_M), and membrane capacitance (C_M) were monitored between each experimental protocol. Recordings were discarded if R_S was >25 MΩ, if R_M was <500 MΩ, or if either changed by >20%. To record action potential firing, *Kiss1*^{ARC} neurons were held at −75 mV, and depolarizing current was injected for 10 ms or 500 ms. To record voltage sags, neurons were held at −75 mV, and hyperpolarizing current was injected for 3 s; the initial hyperpolarization did not differ between groups (Table 1). Spontaneous synaptic currents were recorded at −60 mV for at least 50 s. Data were low-pass filtered (3 kHz) and acquired using an Axopatch 200B amplifier to Spike 2 software (Version 10; Cambridge Electronic Design) via a Micro1401 at a sampling frequency of 20 kHz for offline analysis using Spike 2. DataView (version 12.2.3; Dr. W. J. Heitler, University of St Andrews) was used to measure parameters during single action potentials (Table 1). WinEDR v4.1.5 (Strathclyde Electrophysiology Software) was used to measure sEPSC amplitudes, intervals, and kinetics. RMP, action potential threshold, and minimum voltage (Table 1) have been corrected for a liquid junction potential of −18 mV.

Ovariectomy. Mice were anesthetized and bilaterally ovariectomized. Estrogen implants were placed subcutaneously behind the shoulder to provide 17β-estradiol that was close to the normal diestrus range (28.2 ± 5.6 pg/mL diestrus versus 33.1 ± 6.5 pg/mL OVX + E) for a maximum of 1 wk (29). Following OVX + E, the absence of the estrous cycle in postpuberty mice was confirmed by daily cytological examination of vaginal lavages (48). It should be noted that the stress of surgery could also suppress the estrous cycle. Although the estrogen implants were expected to restore the negative feedback of *Kiss1*^{ARC} neurons, they were more excitable than in intact 6 to 9 wk mice (Fig. 4*C* and Table 1), indicating that the OVX was successful but that the 17β-estradiol did not completely compensate for the loss of ovarian estrogen-mediated negative feedback.

RNA-Seq and Transcriptomics. Transcriptomic studies of fluorescently tagged *Kiss1* neurons were carried out as described previously (49). Female mice aged 3 wk (N = 3) and 10 to 12 wk (metestrus, N = 3 and proestrus, N = 3) were generated by crossing male Kiss1/Cre-GFP mice (47) with female Cg-*Gt(ROSA)26*$^{Sortm6(CAG\text{-}ZsGreen1)Hze}$/J (Jackson Laboratory, IMSR_JAX: 007906). Mice were anesthetized, then perfused transcardially with ice-cold 0.5% formaldehyde in 0.1 M phosphate-buffered saline (PBS; pH 7.4), followed by 20% sucrose solution in PBS. The brains were snap-frozen on dry ice and cryosectioned. Fluorescent neurons (n = 400) from 12 μm-thick sections containing the arcuate nuclei were laser captured and pressure-catapulted into centrifuge tube caps. Microdissections were performed using a Zeiss PALM MicroBeam system (Carl Zeiss Microscopy GmbH, Jena, Germany) operated with PALM RoboSoftware. To ensure sampling consistency, fluorescent neurons were harvested evenly across the entire arcuate nucleus (ARC) from each brain. RNA samples were prepared with the Arcturus Paradise PLUS FFPE RNA Isolation Kit (Applied Biosystems, Waltham, MA). Sequencing libraries were generated with the TruSeq Stranded

Total RNA Library Preparation Gold kit (Illumina, San Diego, CA). A 1 nM library mix (20 μl) was sequenced with an Illumina NextSeq500 instrument using the NextSeq500/550 High Output v2.5 kit (75 cycles). Trimmomatic 0.38 and Cutadapt were used to remove low-quality reads and adapter sequences, respectively, and remaining reads were mapped to the Ensembl mm107 mouse reference genome using STAR (v 2.7.9a). Read assignment to genes, read summarization, and gene-level quantification were performed by featureCounts (Subread v 2.0.2). Differential expression analysis was performed with the DESeq2 R-package. The Ion channel functional category was defined using the KEGG BRITE database.

Cell Dissociation and Quantitative PCR. Tissue punches were taken from the arcuate region of fresh brain slices and incubated with 0.6U papain (Worthington Biochemical Corporation) and 15U DNase at 37 °C for 30 min, washed in Earle's Balanced Salt Solution [containing (2R)-amino-5-phosphonovaleric acid (AP-V)], 0.8 mM kynurenic acid, albumin-ovomucoid inhibitor [3.4% (w/v), 3.47 U/ml DNase, and 5% (w/v) trehalose], then mechanically dissociated. Pools of around twelve fluorescent tdTomato positive cells were collected and stored in DNase-RNase-free H_2O, along with dithiothreitol (0.1 M DTT, ThermoFisher Scientific) and 40 U RNase inhibitor (RiboLock RNase Inhibitor, ThermoFisher Scientific) at −80 °C. Cell pools were converted to cDNA using Superscript™ IV Reverse Transcriptase (ThermoFisher). Both random hexamers and oligo dT were used as primers. In each conversion, one pool of cells was processed as a no-RT-cDNA negative control. Quantitative PCR was conducted using the 2× qPCRBIO SyGreen Mix Lo-ROX (PCRBIOSYSTEMS) on a Quant-Studio™ Real-Time PCR System (ThermoFisher). Quantitation was performed standardized to the house-keeping gene *Tbp* using the ΔΔ Ct method of Pfaffl (50) and relative to the average Ct values of the prepuberty samples.

Statistical Analysis for Electrophysiology and qPCR. Data are presented as mean ± SEM. Using GraphPad Prism (version 9.4.1), a Shapiro–Wilk normality test was used, followed by a *t* test or Mann–Whitney test to compare two groups or a one-way ANOVA (with Dunnett's post hoc test) or Kruskal–Wallis (with Dunn's post hoc test) to compare the effect of one variable on more than two groups of data. A mixed effects analysis or two-way ANOVA (with Sidak's post hoc test) was used to compare the effects of two variables; F and *P* values are given in the Figure Legends. N refers to the number of mice, while n refers to the number of cells (and is equivalent to the number of slices).

Data, Materials, and Software Availability. A version of the accepted manuscript is available (51) along with electrophysiology data (52) in the University of Cambridge Apollo Repository. RNA-seq files are available in BioProject (53) with the accession number PRJNA1262115. Scripts are available on GitHub (54).

ACKNOWLEDGMENTS. WHC was supported by the Ford Physiology Fund Endowment. E.H. was supported by the National Research, Development and Innovation Office of Hungary (K138137).

1. A. Kaprara, I. T. Huhtaniemi, The hypothalamus-pituitary-gonad axis: Tales of mice and men. *Metabolism* **86**, 3–17 (2018).
2. N. de Roux *et al.*, Hypogonadotropic hypogonadism due to loss of function of the KiSS1-derived peptide receptor GPR54. *Proc. Natl. Acad. Sci. U.S.A.* **100**, 10972–10976 (2003).
3. S. B. Seminara *et al.*, The GPR54 gene as a regulator of puberty. *N. Engl. J. Med.* **349**, 1614–1627 (2003).
4. A. K. Topaloglu *et al.*, Inactivating KISS1 mutation and hypogonadotropic hypogonadism. *N. Engl. J. Med.* **366**, 629–635 (2012).
5. L. G. Silveira *et al.*, Mutations of the KISS1 gene in disorders of puberty. *J. Clin. Endocrinol. Metab.* **95**, 2276–2280 (2010).
6. X. d'Anglemont de Tassigny *et al.*, Hypogonadotropic hypogonadism in mice lacking a functional *Kiss1* gene. *Proc. Natl. Acad. Sci. U.S.A.* **104**, 10714–10719 (2007).
7. D. Kumar *et al.*, Murine arcuate nucleus kisspeptin neurons communicate with GnRH neurons in utero. *J. Neurosci.* **34**, 3756–3766 (2014).
8. M. L. Gottsch *et al.*, Molecular properties of Kiss1 neurons in the arcuate nucleus of the mouse. *Endocrinology* **152**, 4298–4309 (2011).
9. M. Alreja, Electrophysiology of kisspeptin neurons. *Adv. Exp. Med. Biol.* **784**, 349–362 (2013).
10. R. Frazao *et al.*, Shift in Kiss1 cell activity requires estrogen receptor alpha. *J. Neurosci.* **33**, 2807–2820 (2013).
11. C. Zhang *et al.*, Molecular mechanisms that drive estradiol-dependent burst firing of *Kiss1* neurons in the rostral periventricular preoptic area. *Am. J. Physiol. Endocrinol. Metab.* **305**, E1384–E1397 (2013).
12. M. Cholanian, S. J. Krajewski-Hall, R. B. Levine, N. T. McMullen, N. E. Rance, Electrophysiology of arcuate neurokinin B neurons in female Tac2-EGFP transgenic mice. *Endocrinology* **155**, 2555–2565 (2014).
13. K. A. Ruka, L. L. Burger, S. M. Moenter, Both estrogen and androgen modify the response to activation of neurokinin-3 and kappa-opioid receptors in arcuate kisspeptin neurons from male mice. *Endocrinology* **157**, 752–763 (2016).
14. R. Piet, S. de Croft, X. Liu, A. E. Herbison, Electrical properties of kisspeptin neurons and their regulation of GnRH neurons. *Front. Neuroendocrinol.* **36**, 15–27 (2015).
15. P. R. F. Mendonca, V. Kyle, S. H. Yeo, W. H. Colledge, H. P. C. Robinson, Kv4.2 channel activity controls intrinsic firing dynamics of arcuate kisspeptin neurons. *J. Physiol.* **596**, 885–899 (2018).
16. J. Qiu *et al.*, Estradiol elicits distinct firing patterns in arcuate nucleus kisspeptin neurons of females through altering ion channel conductances. *eLife* **13**, RP96691 (2024).
17. J. Qiu *et al.*, Estrogenic-dependent glutamatergic neurotransmission from kisspeptin neurons governs feeding circuits in females. *eLife* **7**, e35656 (2018).
18. B. B. Jamieson, R. Piet, Kisspeptin neuron electrophysiology: Intrinsic properties, hormonal modulation, and regulation of homeostatic circuits. *Front. Neuroendocrinol.* **66**, 101006 (2022).
19. C. C. Nestor *et al.*, Evidence of a role for kisspeptin and neurokinin B in puberty of female sheep. *Endocrinology* **153**, 2756–2765 (2012).
20. S. J. Semaan, A. S. Kauffman, Daily successive changes in reproductive gene expression and neuronal activation in the brains of pubertal female mice. *Mol. Cell Endocrinol.* **401**, 84–97 (2015).
21. E. Desroziers, J. D. Mikkelsen, A. Duittoz, I. Franceschini, Kisspeptin-immunoreactivity changes in a sex- and hypothalamic-region specific manner across rat postnatal development. *J. Neuroendocrinol.* **24**, 1154–1165 (2012), 10.1111/j.1365-2826.2012.02317.x.
22. J. Clarkson, A. E. Herbison, Postnatal development of kisspeptin neurons in mouse hypothalamus; sexual dimorphism and projections to gonadotropin-releasing hormone neurons. *Endocrinology* **147**, 5817–5825 (2006).
23. S. Y. Han, T. McLennan, K. Czieselsky, A. E. Herbison, Selective optogenetic activation of arcuate kisspeptin neurons generates pulsatile luteinizing hormone secretion. *Proc. Natl. Acad. Sci. U.S.A.* **112**, 13109–13114 (2015).
24. D. Debanne, Y. Inglebert, M. Russier, Plasticity of intrinsic neuronal excitability. *Curr. Opin. Neurobiol.* **54**, 73–82 (2019).
25. B. P. Bean, The action potential in mammalian central neurons. *Nat. Rev. Neurosci.* **8**, 451–465 (2007).
26. D. Dwivedi, U. S. Bhalla, Physiology and therapeutic potential of SK, H, and M medium afterhyperpolarization ion channels. *Front. Mol. Neurosci.* **14**, 658435 (2021).
27. M. E. Nilsson *et al.*, Measurement of a comprehensive sex steroid profile in rodent serum by high-sensitive gas chromatography-tandem mass spectrometry. *Endocrinology* **156**, 2492–2502 (2015).
28. D. K. Walmer, M. A. Wrona, C. L. Hughes, K. G. Nelson, Lactoferrin expression in the mouse reproductive tract during the natural estrous cycle: Correlation with circulating estradiol and progesterone. *Endocrinology* **131**, 1458–1466 (1992).
29. R. Porteous *et al.*, Reformulation of PULSAR for analysis of pulsatile LH secretion and a revised model of estrogen–negative feedback in mice. *Endocrinology* **162**, bqab165 (2021).
30. V. Matagne, G. Rasier, M. C. Lebrethon, A. Gerard, J. P. Bourguignon, Estradiol stimulation of pulsatile gonadotropin-releasing hormone secretion in vitro: Correlation with perinatal exposure to sex steroids and induction of sexual precocity in vivo. *Endocrinology* **145**, 2775–2783 (2004).
31. A. E. Herbison, Control of puberty onset and fertility by gonadotropin-releasing hormone neurons. *Nat. Rev. Endocrinol.* **12**, 452–466 (2016).
32. P. Campos, A. E. Herbison, Optogenetic activation of GnRH neurons reveals minimal requirements for pulsatile luteinizing hormone secretion. *Proc. Natl. Acad. Sci. U.S.A.* **111**, 18387–18392 (2014).
33. R. A. DeFazio, M. A. Navarro, C. E. Adams, L. S. Milescu, S. M. Moenter, Estradiol enhances the depolarizing response to GABA and AMPA synaptic conductances in arcuate kisspeptin neurons by diminishing voltage-gated potassium currents. *J. Neurosci.* **39**, 9532–9545 (2019).
34. S. de Croft *et al.*, Spontaneous kisspeptin neuron firing in the adult mouse reveals marked sex and brain region differences but no support for a direct role in negative feedback. *Endocrinology* **153**, 5384–5393 (2012).
35. M. Bikson, P. J. Hahn, J. E. Fox, J. G. Jefferys, Depolarization block of neurons during maintenance of electrographic seizures. *J. Neurophysiol.* **90**, 2402–2408 (2003).
36. G. E. Ha, E. Cheong, Spike frequency adaptation in neurons of the central nervous system. *Exp. Neurobiol.* **26**, 179–185 (2017).
37. O. K. Ronnekleiv, J. Qiu, M. J. Kelly, Hypothalamic kisspeptin neurons and the control of homeostasis. *Endocrinology* **163**, bqab253 (2022).
38. P. W. E. Spratt *et al.*, Paradoxical hyperexcitability from Na(V)1.2 sodium channel loss in neocortical pyramidal cells. *Cell Rep.* **36**, 109483 (2021).
39. E. Perez-Reyes, Molecular physiology of low-voltage-activated t-type calcium channels. *Physiol. Rev.* **83**, 117–161 (2003).
40. J. Johnston, I. D. Forsythe, C. Kopp-Scheinpflug, Going native: Voltage-gated potassium channels controlling neuronal excitability. *J. Physiol.* **588**, 3187–3200 (2010).
41. J. Wolfart, J. Roeper, Selective coupling of T-type calcium channels to SK potassium channels prevents intrinsic bursting in dopaminergic midbrain neurons. *J. Neurosci.* **22**, 3404–3413 (2002).
42. J. Yan, R. W. Aldrich, BK potassium channel modulation by leucine-rich repeat-containing proteins. *Proc. Natl. Acad. Sci. U.S.A.* **109**, 7917–7922 (2012).
43. F. Echeverria *et al.*, Large conductance voltage- and calcium-activated K(+) (BK) channel in health and disease. *Front. Pharmacol.* **15**, 1373507 (2024).
44. M. J. Kelly, C. Zhang, J. Qiu, O. K. Ronnekleiv, Pacemaking kisspeptin neurons. *Exp. Physiol.* **98**, 1535–1543 (2013).
45. J. Qiu, Y. Fang, M. A. Bosch, O. K. Ronnekleiv, M. J. Kelly, Guinea pig kisspeptin neurons are depolarized by leptin via activation of TRPC channels. *Endocrinology* **152**, 1503–1514 (2011).
46. A. L. Goddings, A. Beltz, J. S. Peper, E. A. Crone, B. R. Braams, Understanding the role of puberty in structural and functional development of the adolescent brain. *J. Res. Adolesc.* **29**, 32–53 (2019).
47. S. H. Yeo *et al.*, Visualisation of Kiss1 neurone distribution using a Kiss1-Cre transgenic mouse. *J. Neuroendocrinol.* **28**, 12435 (2016).
48. G. Gonzalez, Determining the stage of the estrous cycle in female mice by vaginal smear. *Cold Spring Harb. Protoc.* **2016**, prot094474 (2016).

49. B. Gocz *et al.*, Transcriptome profiling of kisspeptin neurons from the mouse arcuate nucleus reveals new mechanisms in estrogenic control of fertility. *Proc. Natl. Acad. Sci. U.S.A.* **119**, e2113749119 (2022).
50. M. W. Pfaffl, A new mathematical model for relative quantification in real-time RT-PCR. *Nucleic Acids Res.* **29**, e45 (2001).
51. Y. Zhang *et al.*, Neuronal plasticity at puberty in mouse hypothalamic Kiss1 neurons that control fertility. University of Cambridge Apollo Repository. https://doi.org/10.17863/CAM.121772. Deposited 30 September 2025.
52. Y. Zhang *et al.*, Data from "Neuronal plasticity at puberty in mouse hypothalamic Kiss1 neurons that control fertility". University of Cambridge Apollo Repository. https://doi.org/10.17863/CAM.121808. Deposited 30 September 2025.
53. S. Takács, B. Gócz, E. Hrabovszky, Data from "Transcriptomic Profiling of Fluorescently Labeled Kiss1 Neurons from Prepubertal (P22) and from Adult (p70-80) Female Mice of Metestrus and Proestrus Stages." NCBI BioProject. https://www.ncbi.nlm.nih.gov/bioproject?term=PRJNA1262115. Deposited 13 May 2025.
54. S. Takács, B. Gócz, E. Hrabovszky, Scripts for PRJNA1262115. GitHub. https://github.com/goczbalazs/PRJNA1262115. Deposited 13 May 2025.